Eur. Phys. J. B **34**, 155–162 (2003)
DOI: 10.1140/epjb/e2003-00207-3

THE EUROPEAN PHYSICAL JOURNAL B

Magnetism of nanocrystalline Finemet alloy: experiment and simulation

O. Crisan[1,2,a], J.M. Grenèche[3], J.M. Le Breton[4], A.D. Crisan[2], Y. Labaye[3], L. Berger[3], and G. Filoti[1]

[1] National Institute for Materials Physics, PO Box MG-7, 76900 Bucharest, Romania
[2] Department of Physics, Aristotle University of Thessaloniki, 54124 Thessaloniki, Greece
[3] LPEC[b], Université du Maine, 72085 Le Mans Cedex 9, France
[4] GPM[c], Université de Rouen, 76801 Saint Etienne du Rouvray, France

Received 10 April 2003
Published online 4 August 2003 –

Abstract. Mössbauer spectrometry and magnetic measurements are employed to experimentally investigate the magnetic behavior of nanocrystalline $Fe_{73.5}Cu_1Nb_3Si_{13.5}B_9$ ribbons obtained by appropriate annealing of the amorphous precursor. A detailed analysis of the correlation between the microstructure of annealed samples and their magnetic properties is provided. Thermomagnetic data allow the Curie temperatures of both amorphous residual matrix and nanocrystalline phase to be estimated. The differences between Curie temperatures of amorphous residual matrix and amorphous precursor are investigated and explained in terms of magnetic polarization of the matrix by exchange fields arising from the nanocrystalline grains. Theoretical systems of spins consisting of a single ferromagnetic nanocrystalline grain immersed in weakly ferromagnetic environment, quite similar to our real samples, are considered and their magnetic behavior is investigated by Monte Carlo simulation of low temperature spin ordering, with emphasize on the matrix-nanocrystalline grain interface which is shown to exhibit peculiar magnetic behavior. The magnetic features of the matrix-nanocrystalline grain interface are studied, as depending on matrix-nanocrystalline grain exchange coupling as well as crystalline fraction of the nanocrystalline systems.

PACS. 81.07.Bc Nanocrystalline materials – 75.30.-m Intrinsic properties of magnetically ordered materials – 75.75.+a Magnetic properties of nanostructures

1 Introduction

Investigation of soft magnetic materials has received great attention during recent years. Nanocrystalline alloys such as Finemet or Nanoperm have been extensively studied mostly because of their outstanding potential as soft ferromagnets or magnetostrictive materials. The so-called Finemet [1] nanocrystalline $Fe_{73.5}Cu_1Nb_3Si_{13.5}B_9$ ribbons, obtained after subsequent annealing the amorphous precursor, consist of α-Fe(Si) nanocrystalline grains dispersed into an amorphous residual Fe-Nb-B matrix, and exhibit thus excellent soft magnetic properties (high permeability, high saturation magnetization and low magnetostriction). These soft magnetic properties are mostly related to the exchange coupling between nanocrystalline grains, through the amorphous matrix, if the exchange correlation length does not exceed the nanocrystalline grain size [2]. A key issue for understanding how magnetic features of these nanocrystalline Fe-based ribbons is influencing the expected properties for specific applications, is to elucidate the correlation between the microstructural evolution of both the nanocrystalline and amorphous residual phase, and the magnetic behavior of the ribbons. The crystalline volume fraction, as well as the interfaces between nanocrystalline grains and matrix, influences significantly the magnetic properties of these alloys. It has been shown that this interface features a disordered atomic structure and spin-glass-like magnetic behavior [3]. Above the Curie temperature of the amorphous matrix, the magnetic behavior is strongly dependent on the crystalline fraction, *i.e.* the volume ratio between crystalline and amorphous phases. A low crystalline fraction leads to the occurrence of high-temperature superparamagnetic single domain grains while for a high crystalline fraction the paramagnetic intergranular phase is polarized by penetrating fields arising from the nanocrystalline grains [4–7]. The polarization of the amorphous matrix and the interfacial regions by the nanocrystalline grains strongly influences the magnetic behavior of the nanocrystalline alloys, leading to local magnetic correlations between spins.

The paper is structured in two main parts. Firstly, an experimental study of magnetic properties of nanocrystalline Finemet ribbons by Mössbauer spectrometry and

[a] e-mail: crisan@physics.auth.gr
[b] UMR 6087 CNRS
[c] UMR 6634 CNRS

thermomagnetic measurement will be presented. The observed magnetic behavior is correlated with previously obtained structural data on both the microstructure and phase composition [8,9]. Secondly, the magnetic behavior of a single ferromagnetic nanocrystalline grain immersed into a ferromagnetic matrix, by Monte Carlo simulation of low temperature spin ordering will be investigated. The simulation results are then corroborated with experimentally obtained magnetic features.

2 Experimental

The amorphous ribbons with nominal compositions $Fe_{73.5}Cu_1Nb_3Si_{13.5}B_9$ have been prepared by rapid quenching of the melt. Detailed description about the preparation procedure is provided elsewhere [8]. Transmission ^{57}Fe MS spectra were recorded at room temperature with a conventional spectrometer using a ^{57}Co source in a Rh matrix. The isomer shift (relative to metallic α-Fe at room temperature), quadrupolar shift and hyperfine field are denoted δ, ε and B_{hf}, respectively. By Δ is denoted the linewidth (full width at half maximum) of the Mossbauer lines. Estimated errors for the hyperfine parameters originate from the statistical errors σ given by the fitting procedure, taking 3σ. The thermomagnetic measurements were performed with a Faraday balance in the 293–843 K temperature range with a 8 K/min heating rate under an applied field up to 1.5 T.

3 Results and discussions

The initial amorphous state of the as-cast ribbons has been checked both by X-ray diffraction (XRD) and Mössbauer spectrometry. The crystallization behavior has been monitored by differential scanning calorimetry [8]. The recorded scans evidenced the occurrence of small exothermic events prior to primary crystallization at 384 °C and 470 °C, respectively. The temperature of primary crystallization (formation of b.c.c. α-Fe(Si) nanocrystalline phase) is about 522 °C, and other successive exothermic peaks, corresponding to polymorphic crystallization, *i.e.* occurrence of new crystalline phases, such as borides, and/or transformation of metastable intermediate phases, are observed as well.

In order to achieve the nanocrystalline state, the ribbons were submitted to annealing treatments in secondary vacuum to avoid oxidation, at 510 °C for 25 min (A0 sample) and 550 °C for 45 min (A1 sample), respectively. XRD results of the annealed samples have shown that their microstructure consists of body-centered-cubic b.c.c. α-Fe(Si) nanocrystalline grains embedded in the amorphous matrix [8,9]. The average nanocrystalline grain size is determined by the Scherrer's method [10] to be 11 nm and 12 nm for the two annealing treatments, respectively. The lattice parameter of the α-Fe(Si) nanocrystalline phase in our samples, $a = 0.284$ nm, corresponds to a Si content, in the nanocrystalline phase, of about 18 at.%, according to [11].

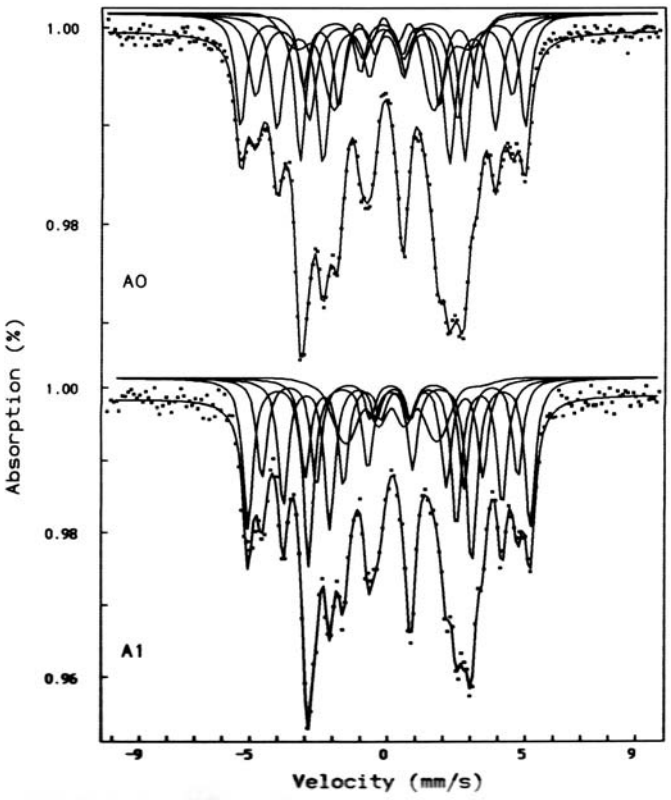

Fig. 1. Room temperature Mössbauer spectra of the annealed A0 and A1 samples. The contributions used for the fittings are shown as well.

3.1 Mössbauer results

The stoechiometric Fe_3Si compound exhibits a DO_3-type structure that consists of two different Fe sites: D sites have 8 nearest-neighbor Fe atoms while A sites have 4 Fe nearest-neighbors and 4 Si nearest-neighbors. Far from the stoechiometry the situation would be rather different. For 8 at% Si, the Si atoms are randomly distributed on the Fe sites in the b.c.c. α-Fe structure. Increasing the Si content up to 25 at%, the value corresponding to Fe_3Si, the compound undergoes a structural phase transition towards an ordered DO_3 structure. For intermediate Si contents, as is the case of the Finemet-type alloys, of 18–20 at%, the structure exhibits several non-equivalent Fe sites, as follows:

(i) the D sites with 8 Fe nearest-neighbors, with a hyperfine field close to that of α-Fe (33 T);
(ii) the A_n sites, where n is the number of Fe nearest-neighbors (n = 4, 5, 6, 7 and 8), the other nearest-neighbors being Si atoms.

It should be mentioned that the hyperfine field of A_n sites decreases with n, with about 4.5–5 T, for every Si atom substituted with Fe. The occupancy of the A_n Fe sites depends on the Si content. Taking into account the Si content obtained from the lattice parameter of the nanocrystalline phase, the ^{57}Fe Mössbauer spectra (Fig. 1) recorded for the two annealed samples have been

Table 1. The hyperfine parameters of the A0 and A1 samples, as resulted from the fit of Mössbauer spectra.

	Sample A0					Sample A1				
	δ	ε	Δ	B_{hf} (T)	A (%)	δ	ε	Δ	B_{hf} (T)	A (%)
Amorphous sextet	0.07	–0.02	0.86	19.1	15	0.06	0.01	0.86	17.9	12
α-Fe(Si): D+A_7+A_8	0.05	0.01	0.46	31.8	23	0.07	–0.02	0.46	31.9	30
α-Fe(Si): A_6	0.08	0.01	0.60	28.6	22	0.08	–0.01	0.57	28.9	18
α-Fe(Si): A_5	0.18	0.00	0.52	24.4	26	0.19	–0.01	0.47	24.7	22
α-Fe(Si): A_4	0.29	0.02	0.43	19.4	14	0.24	–0.02	0.39	20.1	17

Note: δ, Δ (FWHM) and ε are given in mm/s.
The estimated errors are: ±0.09 mm/s for δ; ±0.05 mm/s for ε; ±0.06 mm/s for Δ; B_{hf}; ±0.3 T for B_{hf}; ±1% for A.

fitted with 4 magnetic sextets: D+A_8+A_7, A_6, A_5 and A_4 for the nanocrystalline phase, and one broad magnetic sextet characteristic of topologically disordered materials, ascribed to the amorphous residual matrix. Because of the small difference between the hyperfine fields, the poor resolution of the spectra and the sufficiently high Si content of the samples, leading to small contributions for A_8 and A_7, we have thus chosen to fit the D, A_8 and A_7 contributions on the basis of only one single component. No constraints have been considered between the hyperfine parameters and the fitting results were consistent along all the measured spectra.

Such nanocrystalline alloys are often described as two-phase (amorphous + nanocrystalline) materials. One should take into account that the amorphous intergranular phase is chemically and structurally heterogeneous. It is obvious that a third structural component corresponding to atoms located at the grain surfaces and/or in the interphase boundaries has to be considered since both the local atomic density and the coordination in the boundary regions are different from those of bulk crystalline and amorphous phases. For other classes of nanocrystalline materials (*e.g.* FeZrCuB) besides the magnetic sextet for the nanocrystalline phase (in that case α-Fe) and the low-field hyperfine field distribution for the amorphous phase, a third contribution corresponding to the interfacial regions between nanocrystalline grains and amorphous matrix [3] was introduced to fit the Mössbauer spectra.

Anyway, in our case, due to the complexity of the nanocrystalline structure and to the high spectral overlapping of the different contribution, such a choice would be meaningless, even if it has been shown [3–7] that the interfacial region shows distinct magnetic behavior than the nanocrystalline grains and the amorphous matrix. For our samples, the contribution of the magnetically disordered crystalline interface would be included in the contribution due to nanocrystalline grains.

The fitting parameters, as displayed in Table 1, are consistent for all the measured samples and are in agreement with those found in the literature [12,13]. One should notice first that the relative proportion (denoted by A in Tab. 1) of the amorphous phase slightly decreases for the 550 °C annealed sample, compared to the 510 °C annealed one, as expected. A high relative proportion of the α-Fe(Si) crystalline components (related to the crystalline fraction) is obtained from the MS data (around 87%), but this value takes into account the contribution of both the nanocrystalline phase and the interfacial regions magnetically polarized by penetrating fields from nanocrystalline grains. To estimate the true crystalline fraction, we thus consider that the atomic layer at the nanocrystalline grain surface and the next two successive layers belonging to the matrix form roughly the "boundary" between the crystalline and the amorphous part (≈0.9 nm) Assuming that all the nanocrystalline grains have the same size, *i.e.* the average value deduced from XRD data (5.5 nm radius), a simple calculation leads to the crystalline fraction equal to about 57%, and then to a rough estimation of the magnetically polarized interphase region of about 30% of the sample.

The average hyperfine field of the amorphous matrix decreases with 8%, for A1 compared to A0 sample, according to the residual matrix impoverishing in Fe as the annealing temperature, and consequently the number of α-Fe(Si) crystallites and/or their size, increases. It follows that the hyperfine fields for the 4 α-Fe(Si) components increases with the annealing temperature in average with about 1.5%. The relative proportion of each of the 4 magnetic sextets of α-Fe(Si), related to the Fe sites occupancy, differs for the two annealed samples. This means that during crystallization the Si atoms randomly accommodate the DO_3 sites, depending on the annealing conditions.

3.2 Thermomagnetic data

The magnetic behavior of the annealed samples has been investigated by thermomagnetic measurements. The data were obtained by means of a Faraday balance. This method allows the estimation of the magnetic susceptibility by measuring the Lorentz force acting on the sample under an applied magnetic field. At a given temperature, the susceptibility, can be written as:

$$\chi = \frac{\sigma}{H} + \chi_0 \tag{1}$$

where: χ is the susceptibility, σ the specific magnetization, H the applied field and χ_0 the paramagnetic susceptibility

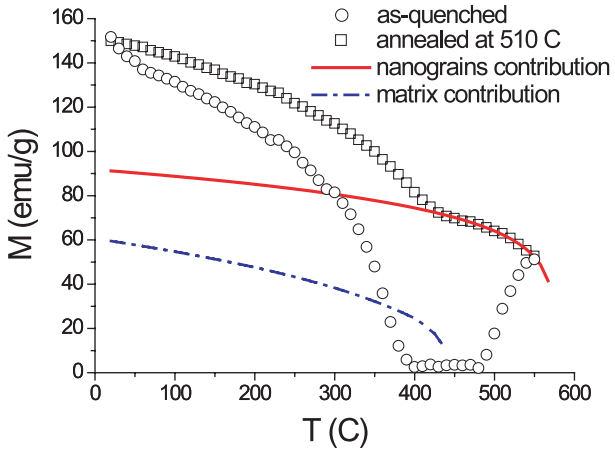

Fig. 2. Specific magnetization *vs.* temperature for as-cast (open circles) and annealed (open squares) A0 sample. The fit according to equation (2) give the matrix (dashed line) and nanocrystalline (continuous line) contributions, respectively.

(zero for ferromagnetic materials). Plotting then $\chi(1/H)$ for four different H values (between 0 and 1.5 T, in our case), one gets a linear dependence whose slope will be the specific magnetization σ.

The specific magnetization *vs.* temperature for both the as-cast sample (open circles) and for the sample annealed at 510 °C (open squares) is presented in Figure 2.

3.2.1 Amorphous precursor

It is well established that the specific magnetization of a single-phase ferromagnet decreases with temperature according to the following Heisenberg-type dependence:

$$\sigma(T) = \sigma(0)\left(1 - \frac{T}{T_C}\right)^{\beta} \qquad (2)$$

where $\sigma(0)$ is the specific magnetization at zero temperature, T_C the Curie temperature and β the critical exponent (typically $\beta = 0.36$ for Heisenberg ferromagnets).

The thermomagnetic curve of the as-quenched sample shows weak ferromagnetic features, typical for the topologically disordered Fe-rich amorphous ribbons, *i.e.* a decrease given by equation (2) of the magnetization towards zero value, at a temperature value T_C corresponding to the Curie point of the amorphous precursor, of about 390 °C. The sample shows zero magnetization up to about 475 °C. Then the magnetization starts to increase. This is due to the onset of crystallization at 475 °C. When the sample begins to crystallize and the number of progressively formed magnetically ordered nanocrystallites increases with the temperature, the nanocrystals net magnetization overcomes the thermally induced spin reversal and the total specific magnetization of the sample increases up to a value corresponding to the end of primary crystallization, point from which the nucleation process has finished ($\approx$ 550 °C from the DSC curves [8]). At higher temperatures, it can be assumed that the magnetization of the as-cast sample vanishes according to equation (2). It is worth noticing the fair agreement between the observed temperature values for both the Curie point of the amorphous and the onset of crystallization, and the temperature values of the pre-crystallization exothermic events observed by DSC analysis [8]. Therefore, the above-mentioned exothermic events observed prior to the crystallization at 384 °C and 470 °C could be unambiguously assigned to the Curie point of the amorphous and the onset of crystallization, respectively.

3.2.2 Nanocrystalline state

The specific magnetization *vs.* temperature curve for the nanocrystalline sample annealed at 510 °C (A0 sample) shows distinct behavior from that of the as-cast sample. It can be seen that increasing the temperature the curve exhibits typical ferromagnetic features – decrease of the specific magnetization due to thermally induced magnetic disorder in the sample – with an inflection point, characteristic for a two-phase behavior, with well separated Curie temperatures, which is usually the case in nanocrystalline alloys. The decrease of magnetization with increasing temperature is slower than in the case of the as-cast amorphous sample and the magnetization values are higher for the nanocrystalline sample than for the amorphous precursor, for any given temperature. It is well established [14,15] that below the observed inflection point the curve comprises the magnetization contribution of the amorphous residual matrix together with the nanocrystalline grains contribution. It should nevertheless be mentioned that in this temperature range the nanocrystals, being ferromagnetically coupled stronger than in the amorphous, have a less important contribution to the magnetization decrease than the amorphous. Above the inflection point, the amorphous contribution to the magnetization vanishes and only the nanocrystals contribute to the net magnetization of the sample. By separating the low temperature profile (contribution of the amorphous phase) from the high temperature profile (contribution of only the nanocrystalline grains) and numerically fitting them to equation (2), one can roughly estimate the Curie temperatures of the amorphous as well as of the nanocrystalline phase. The fittings are showed in Figure 2 by solid line (nanocrystalline contribution) and dashed line (amorphous part), respectively. The amorphous contribution has been obtained by subtraction of nanocrystalline contribution (solid line) from the experimental data, for temperatures below the inflection point. The numerical fitting results shows that the Curie temperature of the α-Fe(Si) nanocrystalline grains is about 590 °C, while the Curie temperature of the residual amorphous is about 440 °C. If we compare this value with that obtained for the amorphous precursor (390 °C), with iron content obviously higher than the amorphous residual matrix, the Curie temperature increases thus of about 12%. This increase is a further indication of the magnetic polarization of the amorphous residual matrix by penetrating

fields arising from nanocrystalline grains. It is expected to be even larger if one compares the amorphous residual matrix with an amorphous as-quenched alloy of identical composition. Some authors [6,16] have reported an increase of T_C with up to 100 K for the amorphous residual matrix compared to the amorphous as-cast samples with identical composition, in the case of Fe-Zr-B-Cu and Fe-Nb-B-Cu (Nanoperm) alloys. However, unlike the Nanoperm alloy, in the case of Finemet nanocrystalline alloys, the exact composition of the amorphous residual matrix is difficult to obtain from Mössbauer data, mainly due to the lack of estimation of the interfacial region. These difficulties could nevertheless be overcome using Monte Carlo simulation, as shown hereafter.

Moreover, by extrapolating the nanocrystalline contribution (high temperature profile) towards low temperatures, one can observe that the initial magnetization value of the nanocrystalline grains $\sigma_{nano}(0)$ is about 90 emu/g while the initial magnetization value for the whole sample $\sigma(0)$ is about 150 emu/g. This indicates a crystalline fraction of 60%, in very good agreement with the estimated crystalline fraction from Mössbauer data (57%) correlated to the assumption that the magnetically polarized interfacial region comprises two atomic layers, successive to the surface layer of the nanocrystalline grain. The correctness of our assumption will get further confirmation from Monte Carlo simulations, in the next section.

3.3 Monte Carlo simulation

The nanocrystalline grain exchange field penetration into the matrix is still an open issue [17–19]. Both temperature dependence of magnetization [3] and ^{57}Fe Mössbauer spectrometry [20] in two-phase nanocrystalline alloys gave evidence for exchange coupling between the grains even above the Curie temperature of the matrix. This exchange field penetration has been also observed and modeled by several authors using random anisotropy concept [21], molecular field approach [18,19] and assuming an exponential decay of exchange interactions through the amorphous matrix [6,16]. It should be noted, anyway, that all these approaches are based on experimental features (either Mössbauer or magnetic measurements) performed on the integrality of the specimens. By using Monte Carlo simulation, one can directly obtain the magnetic behavior of outer shells of the nanocrystalline grain or of the interfacial regions (2–3 successive atomic layers covering the nanocrystalline grain) and their behavior could be correlated with evolution of physical parameters hardly tunable in real materials, such as the matrix-nanocrystalline grain exchange coupling, or surface anisotropy. Indeed, Monte Carlo simulation is a suitable approach to predict behaviors, using simple assumptions such as small and idealized systems, even submitted to extreme conditions which cannot be achieved in laboratories (high magnetic fields).

In the following, the magnetic properties of a single ferromagnetic nanocrystalline grain immersed in a weakly ferromagnetic matrix are studied by means of Monte Carlo simulation of low temperature spin ordering, using the classical Metropolis algorithm [22]. Different contributions to the total magnetization, arising from the core and surface of the nanocrystalline grain, as well as from the interface between the nanocrystalline grain and the matrix and from the matrix itself, can be independently evidenced.

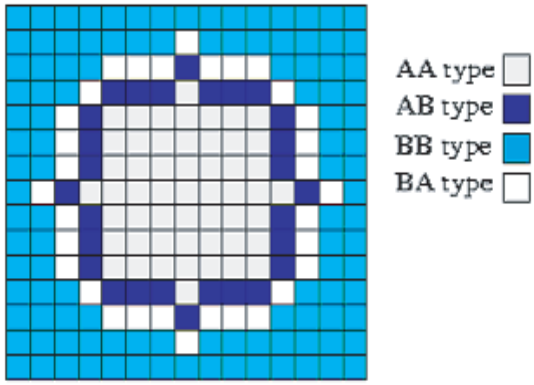

Fig. 3. Structure of the central plane of the 15^3 cubic box which contains the spherical nanocrystalline grain. The AA region corresponds to the nanocrystalline grain core and BB to the matrix. The AB and BA regions correspond, respectively, to the nanocrystalline grain surface and to the matrix-nanocrystalline grain interface.

The system dealt with is a cubic box containing 15^3 sites on a simple cubic lattice. To each site, we assign a classical spin S_i interacting with its six nearest-neighbors *via* an exchange coupling constant J_{ij}. Inside this box, we define a sphere of radius R (in units of the interatomic distance). The sites belonging to the sphere (nanocrystalline grain) are denoted as A sites, while the others, belonging to the matrix, are denoted as B sites. Moreover, we define two non-equivalent atomic layers at the nanocrystalline grain surface: the first one consists of A sites having at least one first-nearest-neighbor of B type and denoted AB, and the other consists of B sites having at least one first-nearest-neighbor of A type, denoted BA. These two atomic shells are assimilated to the nanocrystalline grain surface and to the matrix-nanocrystalline grain interface, respectively. Their magnetic behavior differs from that of the bulk (AA and BB regions). The cross-section of the 15^3 sites cubic box containing a nanocrystalline grain of $R = 6$, with the different regions explained above, is shown in Figure 3. Because of the lower coordination of the sites in the surface leading to a distribution of magnetization over the whole system, one has to consider $J_{\mathrm{AA}} \neq J_{\mathrm{BB}} \neq J_{\mathrm{AB}}$ (for reasons of symmetry $J_{\mathrm{AB}} = J_{\mathrm{BA}}$). The macroscopic thermodynamic properties, such as the temperature dependence of magnetization, specific heat and magnetic susceptibility, are obtained from a Heisenberg-type hamiltonian which contains terms corresponding to exchange and anisotropy energy contributions. The Hamiltonian defined at a given site i reads:

$$H_i = \sum_{j \in V} J_{ij}\, \mathbf{S}_i \cdot \mathbf{S}_j - K_V(\mathbf{S}_{i,V} \cdot \hat{y})^2 - K_S(\mathbf{S}_{i,S} \cdot \hat{n})^2. \quad (3)$$

V is the nearest-neighborhood of site i, J_{ij} are the exchange coupling constants, S_i, S_j the spins corresponding to i and j sites, K the site-dependent anisotropy constant ($K = K_S$ for AB sites and $K = K_V$ elsewhere). For simulation we have chosen a system composed of one ferromagnetic nanocrystalline grain ($J_{AA} > 0$) with strongly coupled spins, embedded in a ferromagnetic environment ($J_{BB} > 0$) with more weakly coupled spins, typical of the amorphous matrix in a nanocrystalline soft magnetic alloy. The size of the nanocrystalline grain ranges from $R = 4$ ($N \approx 268$ sites) to $R = 7$ ($N \approx 1437$ sites). These values correspond to atomic crystalline fractions (number of A sites per total number of sites in the cubic box) of 8% and 43%, respectively. For the system with $R = 7$, the size of the distinctly defined regions is as follows: $N_{\rm AA} = 905$ sites; $N_{\rm AB} = 532$ sites; $N_{\rm BA} = 708$ sites and $N_{\rm BB} = 1230$ sites. We associate the same spin value $S = 1$ to each site. The exchange coupling constants $J_{\rm AA}$ and $J_{\rm BB}$ are taken equal to 3 and 1/2, respectively, while that between the nanocrystalline grain and the matrix $J_{\rm AB}$ ranges from 0.01 (almost decoupled) to 50 (very strong coupling). The unit of J is roughly equivalent to K. The calculations were performed using periodic boundary conditions. The magnetocrystalline anisotropy is uniaxial along the y-axis and equal for the matrix and the nanocrystalline grain core: $K_V = 0.3$. Moreover, we define for the AB region (nanocrystalline grain surface) a surface anisotropy which is oriented normally to the nanocrystalline grain surface, the anisotropy constant being taken in present calculations $K_S = 3.0$.

The temperature dependences of magnetization obtained for different nanocrystalline grain sizes and different $J_{\rm AB}$ values show the two-phase behavior, typical for nanocrystalline soft magnetic alloys. The two contributions that behave distinctly could unambiguously be attributed to the matrix and the nanocrystalline grain. For low temperatures, the magnetization decreases sharply with increasing temperature, typical for weakly coupled ferromagnetic materials, up to a temperature value identified as the Curie temperature of the matrix (hereafter denoted T_C^M). For temperatures higher than T_C^M, the magnetization changes the slope and decreases very slowly, typical for strongly coupled ferromagnetic materials, up to a temperature value identified as the Curie temperature of the nanocrystalline grain (hereafter denoted T_C^N).

In Figure 4 we plot the normalized magnetization *vs.* temperature curves obtained for the system with $R = 7$ equivalent to crystalline fraction $f_{\rm cryst} = 43\%$, considering: (a) $J_{\rm AB} = 2$, and (b) $J_{\rm AB} = 0.01$. The total magnetization as well as the magnetization contributions of all 4 distinctly defined regions is shown. For the almost decoupled system, *i.e.* $J_{\rm AB} = 0.01$, $M_{\rm BB}$ and $M_{\rm BA}$ contributions vanish at T_C^M value as expected, while $M_{\rm AA}$ and $M_{\rm BB}$ contributions vanish at T_C^N. The magnetization values at 0 K are proportional to the volume of each region, since the magnetic moments of all sites have the same value. The total magnetization dependence representing the sum of all contribution does not vanish at T_C^N as expected,

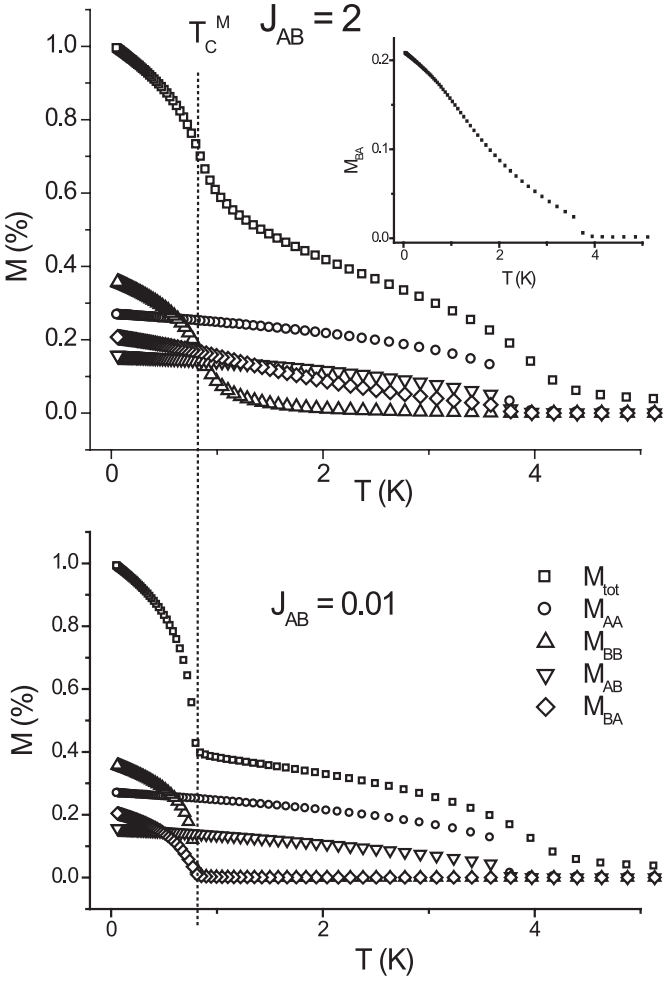

Fig. 4. The total magnetization as well as the contribution to the magnetization of all 4 components (AA, AB, BA and BB) *vs.* temperature for the almost decoupled system $J_{\rm AB} = 0.001$ (bottom) and for the system with $J_{\rm AB} = 2$ (top). The vertical dashed line represents the T_C of the matrix for the almost decoupled system. Inset of upper figure: the interface contribution to the magnetization $M_{\rm BA}$ for the coupled system with $J_{\rm AB} = 2$.

the observed small tail being due to the finite-size effects in our system. Considering now a matrix-nanocrystalline grain coupling $J_{\rm AB} = 2$ (lower than in the crystalline part AA and higher than in the matrix part BB, as is the case in real nanocrystalline materials), one can observe from the $M_{\rm tot}$ and $M_{\rm BB}$ dependences that T_C^M in this case is slightly higher than T_C^M of the almost decoupled system (dashed line in the Fig. 4), indicating a magnetic polarization of the matrix by the exchange coupling in the matrix-nanocrystalline grain interface. $M_{\rm AA}$ and $M_{\rm AB}$ do not vary, indicating a lack of magnetic influence of the interface on the nanocrystalline grain ordering (mainly because $J_{\rm AB} < J_{\rm AA}$). The most interesting behavior is exhibiting by $M_{\rm BA}$ dependence (also shown in inset of Fig. 4). $M_{\rm BA}$ not only vanishes far above T_C^M of the matrix – in fact it vanishes at T_C^N , just as the nanocrystalline grain core and surface contribution, thus providing

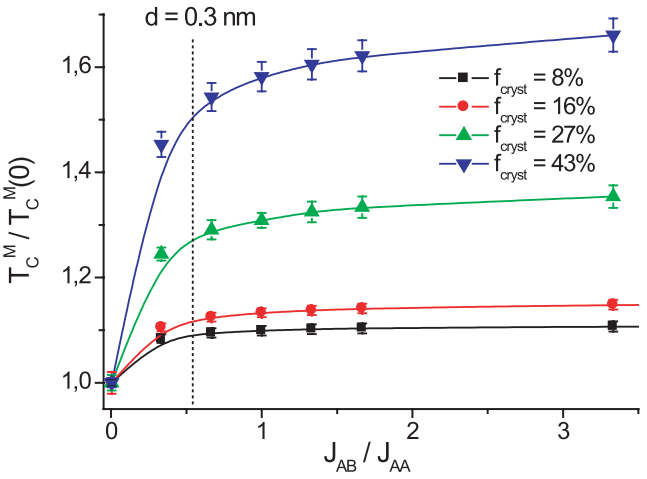

Fig. 5. The increase of T_C of the matrix compared to that of the almost decoupled system (see the text) *vs.* the ratio between matrix-nanocrystalline grain and nanocrystalline grain exchange coupling $J_{\rm AB}/J_{\rm AA}$, for different crystalline fraction.

an increase of its T_C of more than 300% – but also the dependence is far from the expected ferromagnetic profile, exhibiting a rather paramagnetic-like behavior instead. Evidences about paramagnetic behavior of the interface in various nanocrystalline (either Finemet or Nanoperm type) alloys have been reported by several authors [3,19] and explained by boron enrichment of the interface during annealing [19]. As in our simulation, no difference is assumed between atoms in nanocrystalline grain, matrix or interface, this result suggests that the high degree of magnetic disorder (apparent paramagnetism) of the shell considered as matrix-nanocrystalline grain interface, in real materials, could also be due to the difference in exchange coupling values of its neighborhood (weak for the matrix and strong for the nanocrystalline grain) and also to the competition between enhanced surface anisotropy and exchange coupling inside the nanocrystalline grain. A detailed Monte Carlo investigation of the influence of this competition on the equilibrium spin configurations in isolated nanoparticles, has shown that this would give rise to a spin-glass-like configuration in the interfacial region leading to a 'throttled' spin configuration in the nanoparticle core [23].

The above-mentioned observations of T_C^M increase could be made quantitative if plotting the ratio between T_C^M for exchange coupled systems and T_C^M for decoupled system (denoted hereafter $T_C^M(0)$) as a function of $J_{\rm AB}/J_{\rm AA}$ ratio for different crystalline fractions (Fig. 5). One can see the sudden increase of T_C^M for relatively small $J_{\rm AB}/J_{\rm AA}$ values (0.3–0.5), an increase that is sharper as the crystalline fraction is higher. With further increasing of $J_{\rm AB}/J_{\rm AA}$ only slight increase of T_C^M is observed, the curves almost reaching the saturation for $J_{\rm AB}/J_{\rm AA} = 3$. It is worth to mention that the T_C^M values for $J_{\rm AB}/J_{\rm AA} > 1$, have no physical meaning in our case since in the soft magnetic nanocrystalline alloys the matrix is more weakly coupled than the nanocrystalline grains. Nevertheless, the results at high $J_{\rm AB}/J_{\rm AA}$ ratios could be used to predict the behavior of different systems, such as core-shell particles with nonmagnetic core and magnetic shell [24].

Concerning the exchange field penetration into the amorphous matrix, it is generally assumed [6] as following an exponential decay with the distance from the nanocrystalline grains surface:

$$J(d) = J_{\rm core} \exp(-d/l) \tag{4}$$

where: $J(d)$ is the exchange coupling at a distance d from the surface of the nanocrystalline grain, $J_{\rm core}$ is the exchange coupling inside the nanocrystalline grain core ($J_{\rm AA}$) in the case of our simulation) and l is the exchange correlation length. Assuming $l = 5$ Å, typical for this type of materials, and $J_{\rm core} = J_{\rm AA} = 3$, for the interfacial region AB, *i.e.* at about 3 Å from the nanocrystalline grains surface, we obtain the ratio $J(d)/J_{\rm core} \approx 0.55$ (the dashed line in the Fig. 5). Under this assumption, it looks like the simulation using $J_{\rm AB}/J_{\rm AA}$ ratio of 0.55 is in the most reasonable agreement with the situation in real nanocrystalline alloys. It follows that in the interfacial region (at about 3 Å from the nanocrystalline grains surface) the estimated increase for T_C^M is about 50%, for a crystalline fraction of 43%. This increase occurs at a lesser extent for lower crystalline fractions (only 8% for a crystalline fraction of 8%). It is expected that higher nanocrystalline grain size and crystalline fraction would result in further increase of T_C^M and would lead even to a hardening of the magnetism since the nanocrystalline grains would ultimately be in contact.

4 Conclusions and summary

Detailed experimental investigation of the Finemet-type nanocrystalline ribbons, obtained after annealing amorphous precursor, has been performed. ^{57}Fe Mössbauer data have shown that the microstructure obtained after annealing is formed by α-Fe(Si) solid solution dispersed in the residual amorphous matrix, thus confirming the structural analysis. The hyperfine fields corresponding to the different non-equivalent Fe sites in the α-Fe(Si) DO_3-type structure are shown to increase as the crystallization is further promoted at the expenses of the amorphous matrix which becomes impoverished in Fe. The complexity of the nanocrystalline phase in our system, involving the use of multiple magnetic sextets for Mössbauer data analysis, makes meaningless the addition of a supplementary component that should account for the spin-glass-like, highly disordered, matrix-nanocrystalline grain interface. Nevertheless, we have been able to estimate, assuming that two or three successive atomic layers covering the nanocrystalline grain are magnetically polarized by the exchange fields penetrating from the nanocrystalline grains, the crystalline fraction and the interface-to-volume ratio in our samples. The value obtained for the crystalline fraction was remarkably confirmed from thermomagnetic data for the annealed samples. Detailed analysis of the thermomagnetic behavior of both as-cast and annealed

samples allowed us to obtain the Curie temperatures of the amorphous precursor, amorphous residual matrix in the annealed samples and of the nanocrystalline phase. An increase of T_C of about 12% for the amorphous residual matrix compared to that of the amorphous as-cast sample provided evidence for the magnetic polarization of the amorphous residual matrix by penetrating fields arising from nanocrystalline grains. During the crystallization process, small exothermic effects prior to the crystallization (384 °C and 470 °C) have been reported [8]. We have been able to assign these effects, by using the thermomagnetic measurements of the amorphous precursor, to the T_C of the amorphous phase and the onset of crystallization, respectively. Deeper investigations of the magnetic behavior of the matrix-nanocrystalline grain interface have been performed employing the Monte Carlo simulation of low temperature spin ordering, which can give direct insight on the two or three atomic layers at the interface between nanocrystalline grain and matrix. Considering a system composed of a single ferromagnetic nanocrystalline grain immersed into a weakly ferromagnetic environment, quite similar to our real samples microstructure, and a Hamiltonian comprising exchange, magnetostatic and anisotropy terms, we have described the temperature dependence of magnetization of the nanocrystalline grain core, nanocrystalline grain surface, matrix-nanocrystalline grain interface and matrix itself. It has been shown that for intermediate exchange coupling values between the nanocrystalline grain core and matrix values, as is the case in real materials, a significant increase of T_C^M occurs, and this increase is higher as the crystalline fraction in the sample increases. This behavior has been interpreted as a further proof of magnetic polarization of the matrix by the exchange fields arising from nanocrystalline grains. An interesting aspect has been revealed by the magnetic behavior of the first atomic layer successive to the nanocrystalline grain surface. On imposing a slight exchange coupling between nanocrystalline grain and matrix, its magnetization does not vanish at T_C^M for the almost decoupled system but at T_C^N, just like the nanocrystalline grain core and surface and, moreover, its behavior is rather paramagnetic, featuring the high spin disorder at the matrix- nanocrystalline grain interface. More detailed studies are nevertheless imperative to accurately describe the effects of the magnetic polarization of the matrix by the nanocrystalline grains on other macroscopic properties, as is the case of thermal dependence of anisotropy, coercivity and hysteresis.

The authors wish to acknowledge the help of A. Jianu (NIMP) for the synthesis of the ribbons. Part of this work has been performed in the frame of the "Formation Recherche" program 90RO933 no. 152309L, granted by the *Ministère Français des Affaires Étrangères, via* Egide. The financial support of Region Pays de Loire for the postdoctoral position of O.C. at LPEC is gratefully acknowledged. The calculations were performed at the Lotus, a 95 processors Beowulf class, home made parallel computer at LPEC (`http://weblotus.univ-lemans.fr/w3lotus`).

References

1. Y. Yoshizawa, S. Oguma, K. Yamauchi, J. Appl. Phys. **64**, 6044 (1988)
2. G. Herzer, in: *Handbook of Magnetic Materials*, Vol. 10, edited by K.H.J. Buschow (Elsevier Science, 1997)
3. A. Slawska-Waniewska, J.M. Grenèche, Phys. Rev. B **56**, R8491 (1997)
4. A. Hernando, T. Kulik, Phys. Rev. B **49**, 7064 (1994)
5. I. Navarro, M. Ortuno, A. Hernando, Phys. Rev. B **53**, 11656 (1996)
6. J.S. Garitaonandia, D.S. Schmool, J.M. Barandiaran, Phys. Rev. B **58**, 12147 (1998)
7. J.M. Grenèche, M. Miglierini, A. Slawska-Waniewska, Hyp. Int. **126**, 27 (2000)
8. O. Crisan, J.M. Le Breton, G. Filoti, Sensors and Actuators A (in press, 2003)
9. O. Crisan, J.M. Le Breton, A. Jianu, J. Teillet, G. Filoti, J. Alloys Comp. **262-263**, 381 (1997)
10. *X-ray diffraction procedures for polycrystalline and amorphous materials*, edited by H.P. Klug, L.A. Alexander (Wiley, New York, 1974)
11. G. Rixecker, P. Schaaf, U. Gonser, Phys. Stat. Sol. (a) **139**, 309 (1993)
12. G. Hampel, A. Pundt, J. Hesse, J. Phys. Cond. Matt. **4**, 3195 (1992)
13. A. Gupta, N. Bhagat, G. Principi, J. Phys. Cond. Matt. **7**, 2237 (1995)
14. G. Herzer, IEEE Trans. Magn. **25**, 3327 (1989)
15. A. Slawska-Waniewska, M. Gutowski, H.K. Lachowicz, T. Kulik, H. Matyja, Phys. Rev. B **46**, 14594 (1992)
16. A. Hernando, I. Navarro, P. Gorría, Phys. Rev. B **51**, 3281 (1995)
17. A. Hernando, J. Phys. Cond. Matt. **11**, 9455 (1999)
18. A. Hernando, A. González, J. Non-Cryst. Sol. **287**, 256 (2001)
19. A. González, A. Hernando, Phys. Rev. B **65**, 094432 (2002)
20. I. Skorvánek, J. Kovác, J.M. Grenèche, J. Phys. Cond. Matt. **12**, 9085 (2000)
21. K. Suzuki, J.M. Cadogan, Phys. Rev. B **58**, 2730 (1998)
22. *Monte Carlo simulation in statistical physics,* edited by K. Binder, D.W. Heermann (Springer Verlag, Berlin, 1992)
23. Y. Labaye, O. Crisan, L. Berger, J.M. Grenèche, J.M.D. Coey, J. Appl. Phys. **91**, 8715 (2002)
24. N.S. Sobal, M. Hilgendorff, H. Mohwald, M. Giersig, M. Spasova, T. Radetic, M. Farle, Nano Lett. **2**, 621 (2002)